

Minimal Type-I Dirac seesaw and Leptogenesis under A_4 modular invariance

Labh Singh^{1*}, Monal Kashav^{2†}, and Surender Verma^{1‡}

¹Department of Physics and Astronomical Science, Central University of
Himachal Pradesh, Dharamshala-176215, India

²Theoretical Physics Division, Physical Research Laboratory, Navarangpura,
Ahmedabad-380009, India

Abstract

We present a Dirac mass model based on A_4 modular symmetry within Type-I seesaw framework. This extension of Standard Model requires three right-handed neutrinos and three heavy Dirac fermions superfields, all singlet under $SU(2)_L$ symmetry. The scalar sector is extended by the inclusion of a $SU(2)_L$ singlet superfield, χ . Here, the modular symmetry plays a crucial role as the Yukawa couplings acquire modular forms, which are expressed in terms of Dedekind eta function $\eta(\tau)$. Therefore, the Yukawa couplings follow transformations akin to other matter fields, thereby obviating the necessity of additional flavon fields. The acquisition of vev by complex modulus τ leads to the breaking of A_4 modular symmetry. We have obtained predictions on neutrino oscillation parameters, for example, the normal hierarchy for the neutrino mass spectrum. Furthermore, we find that heavy Dirac fermions, in our model, can decay to produce observed baryon asymmetry of the Universe through Dirac leptogenesis.

Keywords: Dirac neutrino; Leptogenesis; Phenomenology; Neutrino mass; Seesaw mechanism.

*sainilabh5@gmail.com

†monalkashav@gmail.com

‡s_7verma@hpcu.ac.in

1 Introduction

In the last two decades several neutrino experiments have confirmed the existence of large leptonic mixing and non-zero neutrino mass. However, there are still three significant questions about neutrino physics that remain unresolved. These questions are (a) neutrino mass hierarchy - whether it's normal hierarchy ($m_1 < m_2 < m_3$) or inverted hierarchy ($m_3 < m_1 < m_2$), and (b) the CP -violation in the leptonic sector, (c) octant degeneracy of atmospheric mixing angle (θ_{23}). The latest global fit analysis discussed in Ref. [1] provides information about the experimental status of various neutrino oscillation observables. Another lingering question pertains to the nature of neutrinos *i.e.* whether they are of Dirac or Majorana type? While the Majorana nature holds theoretical favour, empirical observations to date align with the Dirac nature of neutrinos [2]. The experimental investigations, particularly those concerning neutrinoless double beta ($0\nu\beta\beta$) decay, have yielded null results, which could otherwise confirm the Majorana nature of neutrinos [2].

While the absence of positive outcomes in experiments involving $0\nu\beta\beta$ decay does not definitively establish the Dirac nature of light neutrinos, it does provide significant hints. These hints are substantial enough to formulate scenarios that predict Dirac neutrinos possessing the appropriate mass and mixing properties. Several proposals have been suggested, utilizing additional symmetries such as $U(1)_{B-L}$, A_4 , and Z_N , aimed at producing small Dirac neutrino masses [3–18]. These symmetries play a critical role in preventing the existence of a Majorana mass term ($\bar{\nu}_R^c \nu_R$) among right-handed neutrinos, as well as a tree-level Dirac mass term ($Y_\nu \bar{L} \tilde{\Phi} \nu_R$) between left-handed $SU(2)_L$ doublet and right-handed neutrino field. This prevention is necessary because achieving such a small neutrino mass $m_\nu \lesssim \mathcal{O}(0.1)$ eV would require Yukawa couplings $Y_\nu \lesssim \mathcal{O}(10^{-12})$, which is unnatural. For a detailed review of neutrino mass models based on non-abelian discrete symmetries see [19–22] and references therein. An alternative approach based on modular symmetry was introduced in Ref. [23] as a generalization of discrete symmetry group approach to explain mass and mixing structure of lepton flavors. The later approach has the drawback of being dependent on adhoc symmetry breaking patterns and vacuum alignments acquired by the additional flavon fields present in the scalar sector of the theory. In the former setting, on the other hand, flavor symmetry is realized through nonlinear transformations with minimal and well-defined symmetry breaking pattern. In this approach, all Yukawa couplings are treated as modular forms with even weights, depending on complex modulus τ , which describes the geometry of compactified extra-dimensions in superstring the-

ory. The Lagrangian maintains invariance under the finite modular symmetry group Γ_N . This group, corresponding to a specific value of N , is isomorphic to non-abelian discrete symmetry groups, such as $\Gamma_2 \simeq S_3$ [24–29], $\Gamma_3 \simeq A_4$ [30–45], $\Gamma_4 \simeq S_4$ [46–52], and $\Gamma_5 \simeq A_5$ [53, 54]. However, the overall symmetry will be broken when the modulus τ acquires its vacuum expectation value (vev) rather than the flavons (in non-abelian discrete symmetry approach). Interestingly, very few models exist that have been developed based on higher degree modular forms, also called Siegel Modular forms, unlike the traditional modular forms, which have degree 1. One can find these models devoid of any additional scalar field in the literature [55–58] that explore a unique approach to predict the precise value of neutrino parameters.

Furthermore, the Big Bang nucleosynthesis and cosmic microwave background observations suggest that the Universe contains more baryonic matter than antimatter, often known as matter-antimatter asymmetry. This asymmetry is quantified by the baryon-to-photon ratio, which is estimated to be $\eta_B = (n_B - n_{\bar{B}})/n_\gamma = 6.1 \times 10^{-10}$ [59, 60]. In order to generate this baryon asymmetry dynamically, any theoretical framework must adhere to a set of principles known as the Sakharov conditions [61]. However, these conditions are not satisfied in the Standard Model (SM). Leptogenesis is one beyond SM scenario that has been proposed as a possible explanation for the observed baryon asymmetry in the Universe (BAU) [62]. It operates through the generation of a lepton asymmetry, which, through the $B + L$ violating electroweak sphaleron processes leads to the production of a corresponding baryon asymmetry. Modular symmetry has been successfully employed to explain BAU assuming neutrinos to be of Majorana nature [63–69]. However, in absence of the evidences signaling Majorana nature, alternative avenues have been explored to explain successful baryogenesis with Dirac neutrinos as well [70–79].

In this study, we explore a Dirac mass model employing Type-I seesaw mechanism utilizing A_4 modular symmetry to bypass the need for extra flavon fields in the scalar sector and, in which Yukawa couplings are dictated by complex modulus τ . The SM is extended with the inclusion of right-handed neutrinos, heavy Dirac fermions, and a scalar field, which are singlet under $SU(2)_L$. The fields are assigned modular weights in such a manner that both Majorana and Dirac mass term in the Lagrangian are prohibited. Our model accurately forecasts various parameters of neutrino oscillations and exclusively permits only normal hierarchy for neutrino mass ($m_1 < m_2 < m_3$).

Furthermore, the absence of the lepton-number violating Majorana mass term in our model does not hinder its ability to make predictions regarding baryogenesis through leptogenesis. In our model, the heavy Dirac neutrinos can undergo CP -violating (due to complex modulus

τ) and out-of-equilibrium decay processes into both the left-handed and right-handed lepton sectors, resulting in the generation of equal and opposite asymmetry in both sectors. However, due to the singlet nature of the right-handed neutrino, only the asymmetry in the left sector contributes to baryon symmetry *via* the electroweak sphaleron process. The mechanism is known as Dirac leptogenesis which has been widely explored in the literature using continuous and cyclic symmetries [70–79]. In this work, we have investigated Dirac leptogenesis in the modular symmetry approach for the first time.

The paper is structured as follows: Section 2 provides an overview of the fundamental framework of modular symmetry. In Section 3, we outline the model based on A_4 modular symmetry. Section 4 delves into numerical analysis, yielding predictions on neutrino observables. Section 5 presents the model’s projections regarding Dirac leptogenesis. In Section 6, we summarize the main findings of the present work.

2 Modular Symmetry

The origin of modular symmetries may be attributed to the magnetized extra dimensions, compactification of heterotic strings and D-brane models [80–83, 86]. The modular symmetry provides a novel framework for determining the flavor structure of masses and mixing and are, in general, non-linear realizations of flavor symmetries. The linear flavor symmetries exploit a particular vacuum alignment where symmetry remains unbroken, but in the nonlinear scenario, such a configuration fundamentally doesn’t exist. In vacuum space, the flavor symmetry is broken except some residual fixed points. Each vacuum apart from fixed points holds equal potential as a candidate for describing the fermion spectrum, devoid of bias or preference toward any specific one. For fixed points, the modulus stabilization is needed so that the noval minima can have phenomenological implications [84, 85].

Modular symmetry represents the geometrical symmetry of two dimensional torus defined as Euclidian plane R^2 divided by the lattice Λ . If the lattice (Λ) is spanned by basis vectors $\{e_1, e_2\}$, then complex modulus $\tau = e_2/e_1$ represents a torus structure. Also, Λ can be spanned by the other set of basis $e'_1, e'_2\}$ such as

$$\begin{pmatrix} e'_2 \\ e'_1 \end{pmatrix} = \begin{pmatrix} q & r \\ s & t \end{pmatrix} \begin{pmatrix} e_2 \\ e_1 \end{pmatrix}$$

satisfying the condition $qt - rs = 1$ spanning the group $SL(2, \mathbb{Z})$ isomorphic to modular group

(Γ). The modular group (Γ) consists of linear fractional transformations operating on the complex modulus (τ) upper half-plane such as

$$\gamma : \tau \rightarrow \gamma(\tau) = \frac{q\tau + r}{s\tau + t}, \quad (qt - rs = 1, \text{ with } q, r, s, t \text{ as integers}). \quad (1)$$

The complex number τ serves as a complex modulus with $-0.5 \leq \text{Re}[\tau] \leq 0.5$, $\text{Im}[\tau] > 0$ and $|\tau| \geq 1$ as its fundamental domain. Further, the inhomogeneous modular group $\bar{\Gamma}$ is isomorphic to projective special linear group, $\text{PSL}(2, Z) = \text{SL}(2, Z)/\{I, -I\}$, consisting 2×2 matrices with determinant equal to 1 and q, r, s, t as its elements. The modular transformation is dictated by the S and T transformations $S : \tau \rightarrow -\frac{1}{\tau}$ and $T : \tau \rightarrow (\tau + 1)$ with $S^2 = \mathbb{I}$ and $ST^3 = \mathbb{I}$. The series of modular groups ($\Gamma(N)$) is defined as

$$\Gamma(N) = \left\{ \begin{bmatrix} q & r \\ s & t \end{bmatrix} \in \text{SL}(2, Z), \quad \begin{bmatrix} q & r \\ s & t \end{bmatrix} = \begin{bmatrix} 1 & 0 \\ 0 & 1 \end{bmatrix} \pmod{N} \right\}, \quad (2)$$

where $\Gamma(1) = \text{SL}(2, Z)$. It is important to note that Γ and $-\Gamma$ determine the same linear transformations. The modular group $\bar{\Gamma}(N)$ provides distinct linear transformations such that $\bar{\Gamma} = \bar{\Gamma}(1) = \Gamma(1)/\{I, -I\} = \text{PSL}(2, Z)$. For $N \leq 2$, it may be observed that $\bar{\Gamma}(N) = \Gamma(N)/\{I, -I\}$, and for $N > 2$, $\bar{\Gamma}(N) = \Gamma(N)$. These are, also, referred as the infinite modular groups. The finite modular groups are defined as the quotient group $\Gamma_N = \bar{\Gamma}/\bar{\Gamma}(N)$. The finite modular groups Γ_N are isomorphic to permutation groups, such that $\Gamma_2 \simeq S_3$, $\Gamma_3 \simeq A_4$, $\Gamma_4 \simeq S_4$, and $\Gamma_5 \simeq A_5$. Furthermore, meromorphic functions defined on the upper half of the complex plane preserve their characteristics under all transformations within the modular group such that $f(\gamma\tau) = f(\tau)$, where γ denotes a transformation. Due to restrictive nature of such transformation, we ask for meromorphic functions $f(\tau)$ so that after transformations, $f(\gamma\tau)$ retains the same zeros and poles as $f(\tau)$. Modular forms $f(\tau)$ are holomorphic functions with weight $2k$ and level N , possessing well-defined transformation properties under the group $\Gamma(N)$. For level $N = 3$ and $k \geq 0$,

$$f(\gamma\tau) = (s\tau + t)^{2k} f(\tau). \quad (3)$$

such that modular forms remain invariant under the infinite modular group $\Gamma(3)$ up to a factor of $(s\tau + t)^{2k}$, but they do transform under Γ_3 . Each invariant term should have the vanishing sum of modular weight. With $N = 3$, $\Gamma_3 \simeq A_4$ serves as a non-linear realization of A_4 non-Abelian discrete symmetry. The linear space of modular forms having modular weight $2k$ and level k has dimension $2k + 1$. This results in modular forms for different weights as given in Appendix A.

Symmetry	L_e	L_μ	L_τ	e_R^c	μ_R^c	τ_R^c	ν_{iR}^c	N_{iL}	N_{iR}^c	$\Phi_{u,d}$	χ
A_4	1	$1''$	$1'$	1	$1'$	$1''$	1, $1'$, $1''$	1, $1''$, $1'$	1, $1'$, $1''$	1	1
κ_I	-5	-5	-5	-1	-1	-1	2	1	-1	0	-7

Table 1: Field content and charge assignments of the Type-I Dirac seesaw model under A_4 and κ_I .

\mathbf{Y}_a^b	\mathbf{Y}_1^4	$\mathbf{Y}_{1'}^4$	\mathbf{Y}_1^6
A_4	1	$1'$	1
$-k_I$	4	4	6

Table 2: The higher-order Yukawa couplings transformations within the A_4 modular symmetry.

3 The Model

The field assignments within Type-I Dirac seesaw model, subject to the A_4 modular symmetry in the supersymmetric context, are given in Table 1. The fermionic sector of the SM is extended by three right-handed neutrinos (ν_{iR}^c) and three heavy Dirac fermions (N_{iL}, N_{iR}^c) superfields, all are singlet under $SU(2)_L$ symmetry. The scalar sector is extended by the inclusion of a $SU(2)_L$ singlet superfield χ . We chose charge assignments to the superfields within modular symmetry to disallow the Yukawa term $L\Phi_u\nu_R^c$ and prevent the emergence of Majorana mass term for neutrinos, thereby ensuring Dirac nature of the model. The tensor products of the A_4 group are given in Appendix B. The Feynman diagram representing the Type-I Dirac seesaw is shown in Fig. 1.

The superpotential for the charged leptons is given by

$$\mathcal{W}_l = \alpha(\mathbf{Y}_1^6 L_e \Phi_d e_R^c) + \beta(\mathbf{Y}_1^6 L_\mu \Phi_d \mu_R^c) + \gamma(\mathbf{Y}_1^6 L_\tau \Phi_d \tau_R^c) \quad (4)$$

and the corresponding charged lepton mass matrix is given by

$$M_l = \frac{v_d \mathbf{Y}_1^6}{\sqrt{2}} \begin{pmatrix} \alpha & 0 & 0 \\ 0 & \beta & 0 \\ 0 & 0 & \gamma \end{pmatrix}, \quad (5)$$

where v_d and v_u are the vacuum expectation values (vev) of Higgs superfields Φ_d and Φ_u , respectively (*i.e.* $\langle \Phi_{(u,d)} \rangle = \frac{v_{(u,d)}}{\sqrt{2}}$), and assuming $v_u = v_d$ with $v_\phi = \sqrt{v_u^2 + v_d^2} = 174$ GeV and \mathbf{Y}_1^6 is the Yukawa coupling transforming as singlet under A_4 symmetry with modular weight

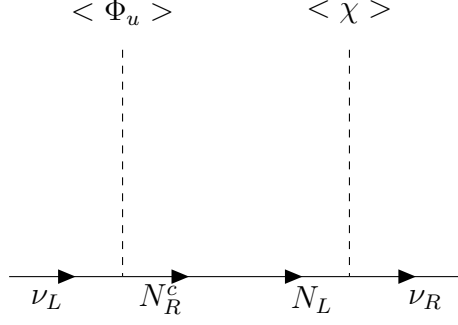


Figure 1: Tree-level Feynman diagram representing generation of neutrino mass in Type-I Dirac seesaw model.

6. Also, the Yukawa Lagrangian of the neutrino sector is given by

$$\begin{aligned}
\mathcal{W}_\nu = & h_1 (\mathbf{Y}_1^6 L_e \Phi_u N_{1R}^c) + h_2 (\mathbf{Y}_1^6 L_\mu \Phi_u N_{2R}^c) + h_3 (\mathbf{Y}_1^6 L_\tau \Phi_u N_{3R}^c) \\
& + h_{11} (\mathbf{Y}_1^4 N_{1L} \chi \nu_{1R}^c) + h_{13} (\mathbf{Y}_{1'}^4 N_{1L} \chi \nu_{3R}^c) + h_{21} (\mathbf{Y}_{1'}^4 N_{2L} \chi \nu_{1R}^c) \\
& + h_{22} (\mathbf{Y}_1^4 N_{2L} \chi \nu_{2R}^c) + h_{32} (\mathbf{Y}_{1'}^4 N_{3L} \chi \nu_{2R}^c) + h_{33} (\mathbf{Y}_1^4 N_{3L} \chi \nu_{3R}^c) \\
& + M_1 N_{1L} N_{1R}^c + M_2 N_{2L} N_{2R}^c + M_3 N_{3L} N_{3R}^c.
\end{aligned} \tag{6}$$

The corresponding Dirac neutrino mass matrices can be written

$$M_D = v_u Y_L = v_u \mathbf{Y}_1^6 \begin{pmatrix} h_1 & 0 & 0 \\ 0 & h_2 & 0 \\ 0 & 0 & h_3 \end{pmatrix}, \quad \text{and} \quad M_{D'} = u Y_R = u \begin{pmatrix} h_{11} \mathbf{Y}_1^4 & 0 & h_{13} \mathbf{Y}_{1'}^4 \\ h_{21} \mathbf{Y}_{1'}^4 & h_{22} \mathbf{Y}_1^4 & 0 \\ 0 & h_{32} \mathbf{Y}_{1'}^4 & h_{33} \mathbf{Y}_1^4 \end{pmatrix}, \tag{7}$$

and the mass matrix for the heavy Dirac fermions is given by

$$M = \begin{pmatrix} M_1 & 0 & 0 \\ 0 & M_2 & 0 \\ 0 & 0 & M_3 \end{pmatrix}, \tag{8}$$

The transformations of the higher-order Yukawa couplings within A_4 modular symmetry are given in Table 2.

In Eqns. (7) and (8), the parameters h_1 , h_2 , and h_3 can be absorbed into h'_{ij} by defining: $h'_{i1} = h_{i1}h_1$, $h'_{i2} = h_{i2}h_2$, and $h'_{i3} = h_{i3}h_3$. The neutrino mass matrix can be obtained from the Type-I Dirac seesaw mechanism [12] given by

$$m_{\nu'} = -M_{D'} M^{-1} M_D, \tag{9}$$

$$= \begin{pmatrix} a & b & c \\ d & e & f \\ g & h & j \end{pmatrix}, \tag{10}$$

where elements of $m_{\nu'}$ are given by

$$\left. \begin{aligned} a &= \frac{h'_{11}{}^2 u^2 v_u^2 (\mathbf{Y}_1^4)^2 (\mathbf{Y}_1^6)^2}{M_1^2} + \frac{h'_{13}{}^2 u^2 v_u^2 (\mathbf{Y}_{1'}^4)^2 (\mathbf{Y}_1^6)^2}{M_3^2}, \\ b &= \frac{h'_{11} h'_{21} u^2 v_u^2 \mathbf{Y}_1^4 (\mathbf{Y}_1^6)^2 \mathbf{Y}_{1'}^4}{M_1^2}, \\ c &= \frac{h'_{13} h'_{33} u^2 v_u^2 \mathbf{Y}_1^4 (\mathbf{Y}_1^6)^2 \mathbf{Y}_{1'}^4}{M_3^2}, \\ d &= \frac{h'_{11} h'_{21} u^2 v_u^2 \mathbf{Y}_1^4 (\mathbf{Y}_1^6)^2 \mathbf{Y}_{1'}^4}{M_1^2}, \\ e &= \frac{h'_{21}{}^2 u^2 v_u^2 (\mathbf{Y}_{1'}^4)^2 (\mathbf{Y}_1^6)^2}{M_1^2} + \frac{h'_{22}{}^2 u^2 v_u^2 (\mathbf{Y}_1^4)^2 (\mathbf{Y}_1^6)^2}{M_2^2}, \\ f &= \frac{h'_{22} h'_{32} u^2 v_u^2 \mathbf{Y}_1^4 (\mathbf{Y}_1^6)^2 \mathbf{Y}_{1'}^4}{M_2^2}, \\ g &= \frac{h'_{13} h'_{33} u^2 v_u^2 \mathbf{Y}_1^4 (\mathbf{Y}_1^6)^2 \mathbf{Y}_{1'}^4}{M_3^2}, \\ h &= \frac{h'_{22} h'_{32} u^2 v_u^2 \mathbf{Y}_1^4 (\mathbf{Y}_1^6)^2 \mathbf{Y}_{1'}^4}{M_2^2}, \\ j &= \frac{h'_{32}{}^2 u^2 v_u^2 (\mathbf{Y}_{1'}^4)^2 (\mathbf{Y}_1^6)^2}{M_2^2} + \frac{h'_{33}{}^2 u^2 v_u^2 (\mathbf{Y}_1^4)^2 (\mathbf{Y}_1^6)^2}{M_3^2}. \end{aligned} \right\} \quad (11)$$

We define the Hermitian neutrino mass matrix as

$$m_\nu \equiv m_{\nu'} m_{\nu'}^\dagger = \begin{pmatrix} a^2 + b^2 + c^2 & ad + be + cf & ag + bh + cj \\ ad + be + cf & d^2 + e^2 + f^2 & dg + eh + fj \\ ag + bh + cj & dg + eh + fj & g^2 + h^2 + j^2 \end{pmatrix}. \quad (12)$$

In the following section, we perform numerical analysis and explore the model's prediction for various neutrino oscillation observables utilizing the diagonalization constraints of neutrino mass matrix given in Eqn. (12).

4 Numerical Analysis and Discussion

In numerical analysis, the real coupling constants, which are free parameters in the model, are randomly varied within the range:

$$h'_{ij} \in (-1, 1) \quad \text{and} \quad \alpha, \beta, \gamma \in (0, 1). \quad (13)$$

In addition, the Yukawa couplings entering in Y_L and Y_R (in Eqn. (7)) depend on complex modulus τ . The real and imaginary components of τ are randomly varied within the fundamental

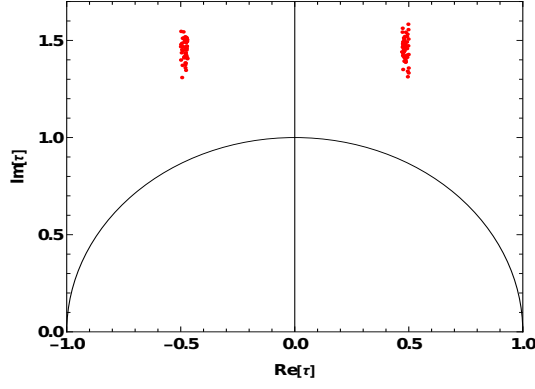


Figure 2: The parameter space of real and imaginary parts of complex modulus τ within the fundamental domain.

domain, $-0.5 \leq \text{Re}[\tau] \leq 0.5$ and $\text{Im}[\tau] > 0$. The *vev* of singlet scalar field χ is varied randomly in the range $(1 - 10^6)$ GeV. In order to determine the masses of the active light neutrinos (m_1, m_2, m_3) , we have performed numerical diagonalization of the neutrino mass matrix (m_ν) given in Eqn. (12). The Hermitian neutrino mass matrix m_ν can be, in general, diagonalized by unitary mixing matrix U , viz., $U m_\nu U^\dagger = \text{diag}(m_1^2, m_2^2, m_3^2)$. The neutrino mixing matrix U can be parameterized in terms of three mixing angles $(\theta_{12}, \theta_{13}, \theta_{23})$ and one Dirac-type CP -violating phase (δ) in the charged lepton basis

$$U = \begin{pmatrix} c_{12}c_{13} & s_{12}c_{13} & s_{13}e^{-i\delta} \\ -s_{12}c_{23} - c_{12}s_{23}s_{13}e^{i\delta} & c_{12}c_{23} - s_{12}s_{23}s_{13}e^{i\delta} & s_{23}c_{13} \\ s_{12}s_{23} - c_{12}c_{23}s_{13}e^{i\delta} & -c_{12}s_{23} - s_{12}c_{23}s_{13}e^{i\delta} & c_{23}c_{13} \end{pmatrix} = \begin{pmatrix} U_{11} & U_{12} & U_{13} \\ U_{21} & U_{22} & U_{23} \\ U_{31} & U_{32} & U_{33} \end{pmatrix}, \quad (14)$$

where $c_{ij} = \cos \theta_{ij}$ and $s_{ij} = \sin \theta_{ij}$ and δ is Dirac-type CP -violating phase. Further, the neutrino mixing angles can be determined from the unitary matrix U using the following relations

$$\sin^2 \theta_{13} = |U_{13}|^2, \quad \sin^2 \theta_{23} = \frac{|U_{23}|^2}{1 - |U_{13}|^2}, \quad \sin^2 \theta_{12} = \frac{|U_{12}|^2}{1 - |U_{13}|^2}. \quad (15)$$

Also, the degree of CP -violation quantified using Jarlskog invariant [87, 88] is defined as

$$J_{CP} = \text{Im}[U_{11}U_{22}U_{12}^*U_{21}^*] = s_{12}c_{12}s_{23}c_{23}s_{13}c_{13}^2 \sin \delta. \quad (16)$$

This process yielded predictions on the neutrino mixing angles and CP -violation (δ) using Eqns. (15) and (16), respectively. In Fig. 2, we have shown the allowed parameter space of τ in the complex plane. It can be seen from Fig. 2 that $\text{Im}[\tau]$, which is responsible for CP -violation in the model, assumes values slightly greater than 1 while the $\text{Re}[\tau]$ has values

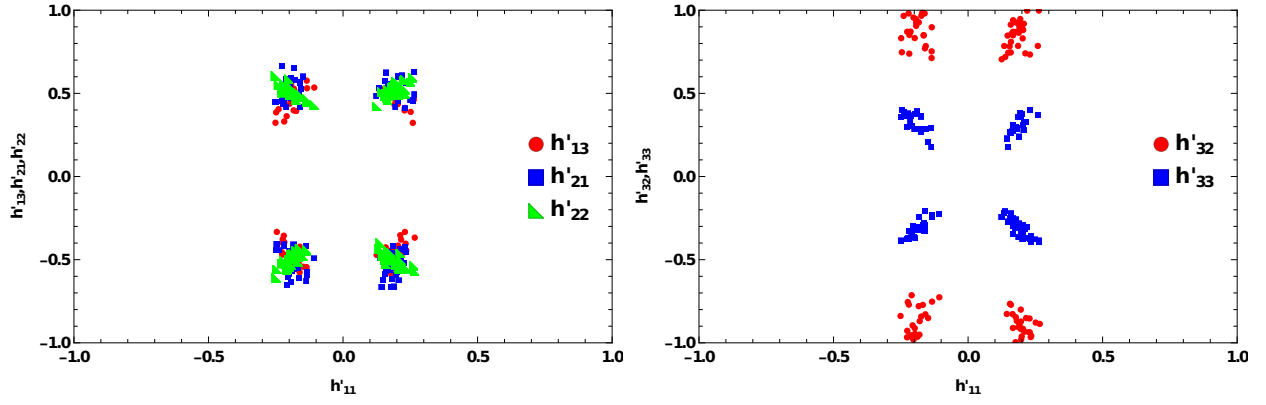


Figure 3: Allowed ranges of parameters h'_{ij} from the neutrino oscillation data shown in Table 3.

Parameter	best-fit $\pm 1\sigma$ range (NH)	best-fit $\pm 1\sigma$ range (IH)	3σ range (NH)	3σ range (IH)
$\sin^2 \theta_{12}$	$0.304^{+0.013}_{-0.012}$	$0.304^{+0.012}_{-0.012}$	0.269-0.343	0.269-0.343
$\sin^2 \theta_{23}$	$0.573^{+0.018}_{-0.023}$	$0.578^{+0.017}_{-0.021}$	0.405-0.624	0.410-0.623
$\sin^2 \theta_{13}$	$0.02220^{+0.00068}_{-0.00062}$	$0.02238^{+0.00064}_{-0.00062}$	0.02060-0.02435	0.02053-0.02434
$\frac{\Delta m_{23}^2}{10^{-3} \text{eV}^2}$	$2.515^{+0.028}_{-0.028}$	$2.498^{+0.028}_{-0.029}$	2.431-2.598	-2.584- -2.413
$\frac{\Delta m_{12}^2}{10^{-5} \text{eV}^2}$	$7.42^{+0.21}_{-0.20}$	$7.42^{+0.21}_{-0.20}$	6.82-8.04	6.62-8.04

Table 3: The neutrino oscillation data from global fit is used in the numerical analysis [1].

near ± 0.5 . Also, Fig. 3 depicts the allowed ranges of the free parameters h'_{ij} constrained by neutrino oscillation data given in Table 3. Further, Fig. 4 illustrates the model's prediction regarding the neutrino mixing angles. It is apparent from Fig. 4 that all the mixing angles fall within the 3σ experimental range given in Table 3 for NH. The value of the sum of neutrino masses lies in the range $0.088 \text{ eV} \leq \sum m_\nu \leq 0.105 \text{ eV}$ which is below the cosmological bound on the sum of neutrino masses $\sum m_\nu < 0.12 \text{ eV}$ [59]. Fig. 5 illustrates the correlation between δ and J_{CP} . The CP -violating phase δ is constrained to the first and fourth quadrants with the normal hierarchy (NH) only, consistent with the T2K experiment (prefer NH) at 3σ with nearly maximal CP -violations [89–91]. We, also, explored the parameter space pertaining to the inverted hierarchy (IH) of neutrino masses. The model ruled out the IH at 3σ confidence level as evident in Fig. 6. The atmospheric mixing angle ($\sin^2 \theta_{23}$) and reactor mixing angle ($\sin^2 \theta_{13}$) falls outside 3σ experimental range (Fig. 6), though the values of the solar mixing angle ($\sin^2 \theta_{12}$) are consistent with 3σ experimental ranges given in Table 3.

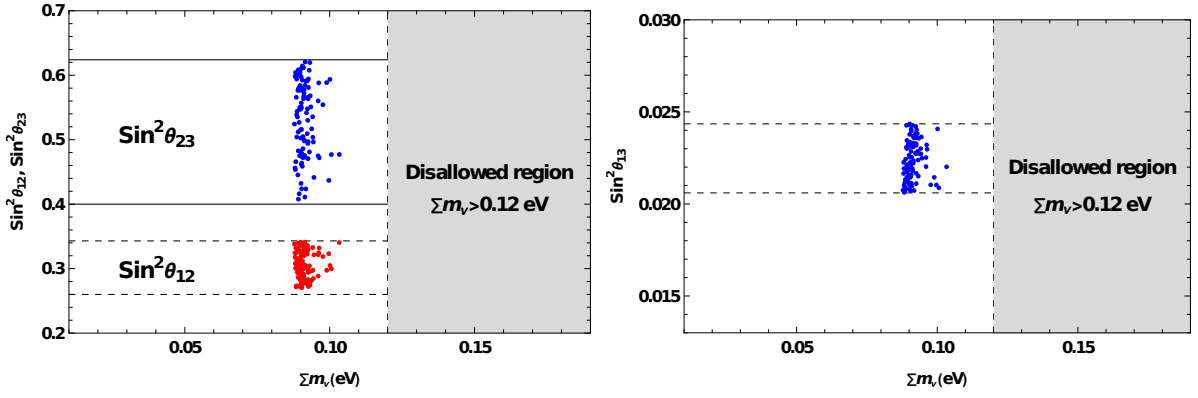


Figure 4: **Left:** Correlation plot between $(\sin^2 \theta_{12}, \sin^2 \theta_{23} - \sum m_\nu)$, **Right:** Correlation plot between $(\sin^2 \theta_{13} - \sum m_\nu)$, for NH.

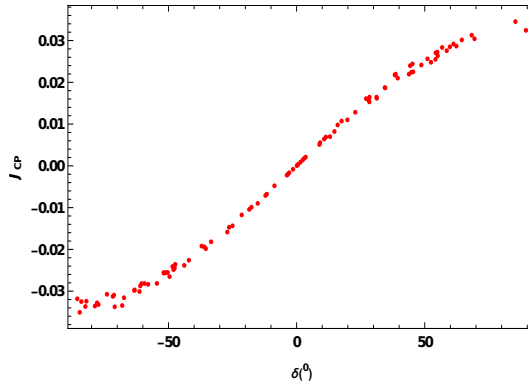


Figure 5: Correlation plot between $(\delta - J_{CP})$.

5 Dirac Leptogenesis

In this model, the lepton number conservation ensures the absence of any net lepton asymmetry. However, it is feasible to induce an equal and opposite lepton asymmetry within both left and right-handed lepton sectors ($\eta_{\Delta L} = -\eta_{\Delta \nu_R}$) through out-of-equilibrium and CP -violating decays ($N \rightarrow L\Phi$ and $N \rightarrow \nu_R\chi$) involving the heavy Dirac fermions N_i . Subsequently, the electroweak sphaleron processes [92] facilitate the conversion of the asymmetry in the left-lepton sector into the baryon asymmetry before the electroweak phase transition. Conversely, the asymmetry in the right-lepton sector cannot be converted into baryon asymmetry due to the singlet nature of the right-handed neutrinos. We have considered the scenario wherein supersymmetry is broken at a higher mass scale exceeding the mass scale of heavy Dirac fermions (N_i) in our model. This ensures that we need not account for the contribution of superparticles to the final baryon asymmetry [93,94]. In the analysis, we have considered scale of N_1 to be $\mathcal{O}(10^{12})$ GeV, to have leptogenesis in the unflavored regime [95–98]. Fig. 7 illustrates the relevant decay channels of

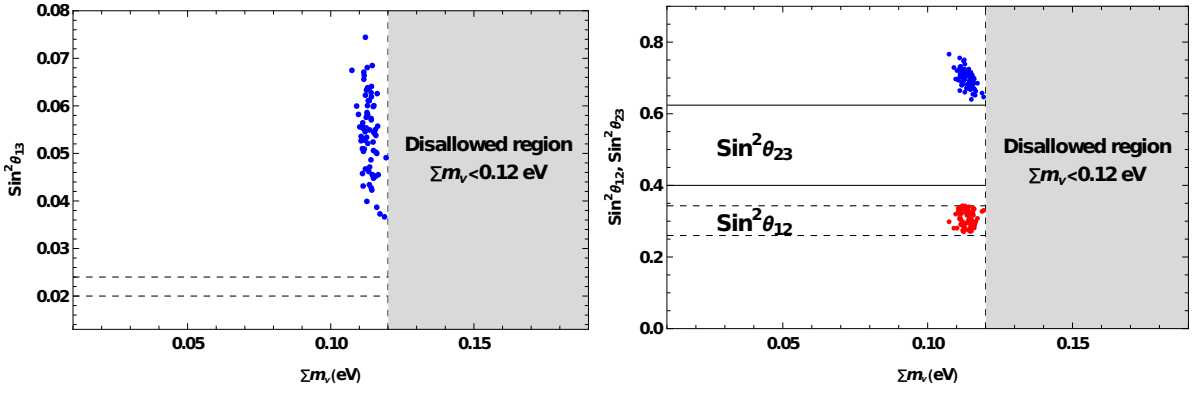


Figure 6: **Left:** Correlation plot between $(\sin^2 \theta_{13} - \sum m_\nu)$, **Right:** Correlation plot between $(\sin^2 \theta_{12}, \sin^2 \theta_{23} - \sum m_\nu)$, for IH.

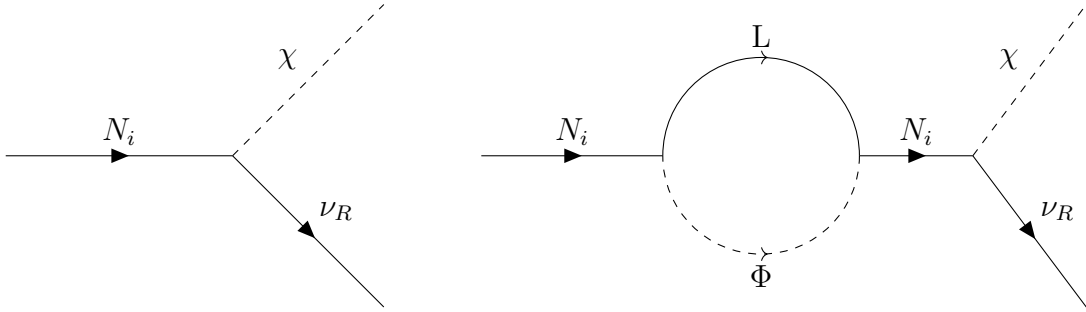


Figure 7: Tree-level (left) and 1-loop self-energy (right) Feynman diagram for the decays of N .

the N_i . The CP asymmetry parameter for the right-sector is given as [99]

$$\epsilon = \frac{\sum_k (\Gamma(N_i \rightarrow \nu_{Rk}\chi) - \Gamma(\bar{N}_i \rightarrow \bar{\nu}_{Rk}\chi^*))}{\sum_j \Gamma(N_i \rightarrow \nu_{Rj}\chi) + \sum_l \Gamma(N_i \rightarrow L_l\Phi)} \quad (17)$$

which can be simplified as

$$\epsilon \simeq -\frac{1}{8\pi} \frac{M_1}{v_u u} \frac{\text{Im}[(Y_L m_\nu^\dagger Y_R)_{11}]}{(Y_L Y_L^\dagger)_{11} + (Y_R^\dagger Y_R)_{11}}. \quad (18)$$

The couplings Y_L and Y_R are functions of complex modulus τ *via* modular forms \mathbf{Y}_1^6 and $(\mathbf{Y}_1^4, \mathbf{Y}_1^4)$, respectively (refer to Appendix A). It is possible to create a net baryon asymmetry if net lepton asymmetry is generated prior to the sphaleron decoupling epoch. However, in order to impede the left-sector lepton asymmetry from being washed out, it is important to prevent the equilibration of left and right-sectors, leading to condition

$$\Gamma_{L-R} \sim \frac{|Y_L|^2 |Y_R|^2 T^3}{M_1^2} < H(T), \quad \text{where} \quad H = 1.67 \frac{\sqrt{g_*}}{M_{pl}} T^2 \text{ is Hubble constant,} \quad (19)$$

and g_* is the effective number of relativistic degree of freedom and M_P is the Planck mass, $M_P = 1.2 \times 10^{19}$ GeV.

In order to realise the baryogenesis through Dirac leptogenesis in our model, we follow the scheme given in Ref. [99]. The relevant Boltzmann equations for the Dirac leptogenesis are

Benchmark Point (BP)	M_1 (GeV)	u (GeV)	Complex modulus τ
BP1	10^{12}	10^3	$-0.4980 + 1.5464i$
BP2	10^{12}	10^4	$0.4814 + 1.5005i$
BP3	10^{12}	10^5	$-0.4871 + 1.5123i$

Table 4: The benchmark points utilised to produce the lepton asymmetry in the model via Dirac leptogenesis. The Yukawa couplings corresponding to BPs are given in Eqn. (??).

given by

$$\left. \begin{aligned} \frac{d\eta_{\Sigma N_1}}{dz} &= \frac{z}{H(z=1)} \left[2 - \frac{\eta_{\Sigma N_1}}{\eta_{N_1}^{eq}} + \epsilon \left(\frac{3\eta_{\Delta L}}{2} + \eta_{\Delta L} \right) \right] \Gamma^D, \\ \frac{d\eta_{\Delta N_1}}{dz} &= \frac{z}{H(z=1)} \left[\eta_{\Delta L} - \frac{\eta_{\Delta N_1}}{\eta_{N_1}^{eq}} - B_R \left(\frac{3\eta_{\Delta L}}{2} + \eta_{\Delta N_1} \right) \right] \Gamma^D, \\ \frac{d\eta_{\Delta L}}{dz} &= \frac{z}{H(z=1)} \left\{ \left[\epsilon \left(1 - \frac{\eta_{\Sigma N_1}}{2\eta_{N_1}^{eq}} \right) - \left(1 - \frac{B_R}{2} \right) \left(\eta_{\Delta L} - \frac{\eta_{\Delta N_1}}{\eta_{N_1}^{eq}} \right) \right] \Gamma^D - \left(\frac{3\eta_{\Delta L}}{2} + \eta_{\Delta N_1} \right) \Gamma^W \right\} \end{aligned} \right\} \quad (20)$$

where $\eta_{\Sigma N} = \frac{\eta_N + \eta_{\bar{N}}}{\eta_\gamma}$, $\eta_{\Delta N} = \frac{\eta_N - \eta_{\bar{N}}}{\eta_\gamma}$, $z = \frac{M_{N_1}}{T}$ and

$$\Gamma^D = \frac{z^2}{2} K_1(z) [\Gamma(N_1 \rightarrow L\Phi) + \Gamma(N_1 \rightarrow \nu_R \chi)] = \Gamma^W. \quad (21)$$

It is to be noted that the Boltzmann equations given in Eqn. (20) are, in general, function of complex modulus τ through ϵ , branching ratio (B_R) and Γ_D or Γ_W . The electroweak sphaleron processes convert the net lepton asymmetry in the left-sector to the baryon asymmetry by a conversion factor given by

$$\eta_B = -\frac{28}{79}\eta_{\Delta L}. \quad (22)$$

The allowed parameter space of vacuum alignment u of singlet scalar χ and complex modulus τ have been obtained by requiring consistent low energy neutrino phenomenology in the model. Three such values of u and τ are given as BPs of the model in Table 4. With the evolution of the Universe, the heavy Dirac fermion begins to decay to SM particles, which leads to an increase in the comoving number density of lepton asymmetry ($\eta_{\Delta L}$). In the numerical analysis, the evolution of $\eta_{\Delta L}$ has been studied using coupled Boltzmann equations given in the Eqn. (20) for the three BPs (Table 4). It can be deduced from Eqns. (7) and (9) that for smaller values of u one requires larger Yukawa couplings, or vice-versa, to satisfy neutrino phenomenology. It is to be noted that as we go from BP1 to BP3, u is increasing from 10^3 to 10^5 GeV.

In order to calculate the baryon asymmetry through Dirac leptogenesis in the model, we assume $(Y_L Y_L^\dagger)_{11} = (Y_R^\dagger Y_R)_{11}$. In Fig. 8, we have depicted the evolution of the comoving number density

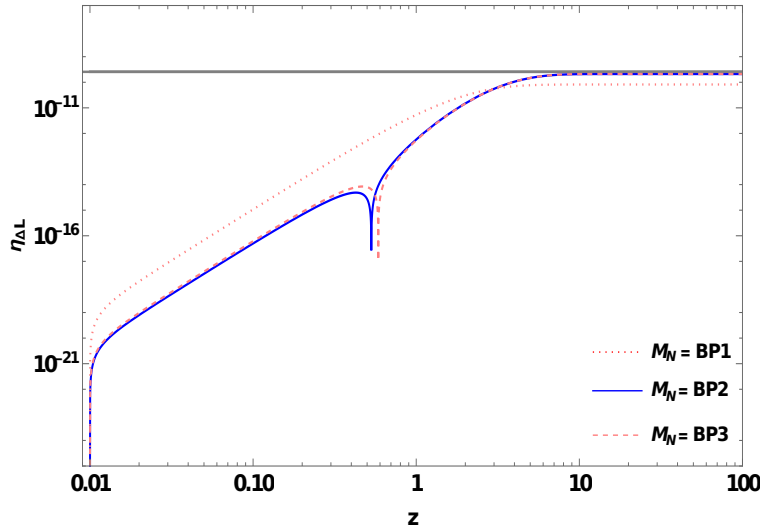


Figure 8: The evolution of comoving number density of lepton asymmetry with $z = M_{N_1}/T$ for different benchmark points given in Table 4. The required asymmetry in the lepton sector is represented by the solid horizontal line, which is then converted to the required baryon asymmetry through the electroweak sphaleron action.

of the lepton asymmetry as a function of $z \equiv M_{N_1}/T$. The larger Yukawa coupling (smaller u) while generating lepton asymmetry shall enhance washout scattering processes (Γ_W) as well which has been shown in Fig. (8) with dotted-red curve. However, as discussed earlier, the larger u induces smaller Yukawa couplings which in turn diminishes washout effects culminating in the saturation of lepton asymmetry (blue and dashed-pink curves), near $z \approx 6$, consistent with observed value of $\eta_{\Delta L}$. The resulting lepton asymmetry transforms into the baryon asymmetry through the $B + L$ violating electroweak sphaleron process, as given in Eqn. (22).

6 Conclusions

In summary, absence of evidences, pointing towards Majorana nature of neutrinos, have motivated theoretical investigations explaining non-zero neutrino mass and BAU considering neutrino to be Dirac particle. The baryogenesis *via* leptogenesis have been widely discussed within flavor symmetries, discrete or cyclic, for recent review see [21] and references therein. These frameworks, sometimes lacks justification for adhoc symmetry breaking patterns and vacuum alignments acquired by the additional flavon fields in the scalar sector of the model. The recent investigations, in this direction, have focused on modular symmetry wherein flavor symmetry is realized through non-linear transformations with minimal and well defined symmetry breaking

pattern. In this work, we have proposed a scenario of neutrino mass generation explaining, simultaneously, the low energy neutrino phenomenology and BAU, assuming Dirac nature of neutrino.

In particular, we have investigated a Dirac mass model incorporating A_4 modular symmetry within the Type-I seesaw framework to elucidate neutrino phenomenology and account for observed oscillation data. The SM fermionic sector is extended by three right-handed $SU(2)_L$ singlets and three heavy Dirac fermionic superfields, while its scalar sector is augmented by a scalar superfield singlet under $SU(2)_L$ gauge symmetry. Choosing the appropriate charge assignment under A_4 modular symmetry, prevents the tree-level Dirac and Majorana mass terms, facilitating the construction of neutrino mass matrix within Type-I Dirac seesaw. The Yukawa couplings are related to the modular forms under A_4 modular symmetry. The invariance under A_4 modular symmetry is broken by the *vev* of the complex modulus τ . We have explored the allowed parameter space of the model in light of global neutrino oscillation data. The model predicts normal hierarchical neutrino mass spectrum which is in consonance with the recent observation from T2K experiment. In general, the complex modulus τ ($\text{Im}(\tau)$) seeds CP violation and lepton asymmetry resulting in baryon asymmetry consistent with the observed BAU. We, also, find that the Dirac-type CP -violating phase δ lie in the range, $(-90^\circ - 90^\circ)$. The CP -violating and out-of-equilibrium decay of heavy Dirac fermions produces equal and opposite lepton asymmetry in both the left and right-handed lepton sectors. However, due to the singlet nature of the right-handed neutrino, asymmetry in the left-handed-lepton sector converted *via* $B + L$ violating the electroweak sphaleron process to the baryon asymmetry of the Universe. In order to study the evolution of the lepton asymmetry, we solve the coupled Boltzmann equations for three BPs. For higher Yukawa coupling, washout effects increase, thereby limiting the lepton asymmetry below the experimentally required value. However, for smaller Yukawa couplings, washout effects get diminished and lepton asymmetry saturates around its observed value as shown in Fig. 8.

Acknowledgments

LS acknowledges financial support provided by Council of Scientific and Industrial Research (CSIR) vide letter No. 09/1196(18553)/2024-EMR-I. MK would like to acknowledge Physical Research Laboratory, Ahmedabad, Govt. of India for the Post-Doctoral Fellowship vide letter No. PRL/ADMN/MK/2023.

A Modular forms corresponding to $\Gamma_3 = A_4$

The Dedekind eta-function, defined in the upper complex plane, constructs modular forms of weight 2 and level 3, given as

$$\eta(\tau) = q^{1/24} \prod_{n=1}^{\infty} (1 - q^n)$$

with $q = e^{i2\pi\tau}$, and written in terms of the $\eta(\tau)$ and its derivative as

$$\left. \begin{aligned} Y_1(\tau) &= \frac{i}{2\pi} \left[\frac{\eta'(\tau/3)}{\eta(\tau/3)} + \frac{\eta'((\tau+1)/3)}{\eta((\tau+1)/3)} + \frac{\eta'((\tau+2)/3)}{\eta((\tau+2)/3)} - \frac{27\eta'(3\tau)}{\eta(3\tau)} \right], \\ Y_2(\tau) &= -\frac{i}{\pi} \left[\frac{\eta'(\tau/3)}{\eta(\tau/3)} + \omega^2 \frac{\eta'((\tau+1)/3)}{\eta((\tau+1)/3)} + \omega \frac{\eta'((\tau+2)/3)}{\eta((\tau+2)/3)} \right], \\ Y_3(\tau) &= -\frac{i}{\pi} \left[\frac{\eta'(\tau/3)}{\eta(\tau/3)} + \omega \frac{\eta'((\tau+1)/3)}{\eta((\tau+1)/3)} + \omega^2 \frac{\eta'((\tau+2)/3)}{\eta((\tau+2)/3)} \right], \end{aligned} \right\} \quad (23)$$

where $\omega = e^{i2\pi/3}$. They fulfil the condition

$$Y_2^2 + 2Y_1Y_3 = 0.$$

These three modular forms, arranged as $\mathbf{Y}_3^2 = \begin{pmatrix} Y_1 & Y_2 & Y_3 \end{pmatrix}$ in the $\mathbf{3}$ irreducible representation of A_4 , with indices denoting weight and multiple ($\mathbf{Y}_{\text{multiplet}}^{\text{weight}}$), facilitate construction of higher-weight modular forms using tensor products of A_4 . For $k = 4$, there are 5 linearly independent modular forms, arranged into two singlets $\mathbf{1}, \mathbf{1}'$ and one triplet $\mathbf{3}$ of A_4 :

$$\mathbf{Y}_1^4 = Y_1^2 + 2Y_2Y_3, \quad \mathbf{Y}_{1'}^4 = Y_3^2 + 2Y_1Y_2, \quad \mathbf{Y}_3^4 = \begin{pmatrix} Y_1^2 - Y_2Y_3 \\ Y_3^2 - Y_1Y_2 \\ Y_2^2 - Y_1Y_3 \end{pmatrix}.$$

For $k = 6$, one has

$$\mathbf{Y}_1^6 = Y_1^3 + Y_2^3 + Y_3^3 - 3Y_1Y_2Y_3, \\ \mathbf{Y}_{3,1}^6 = (Y_1^2 + 2Y_2Y_3) \begin{pmatrix} Y_1 \\ Y_2 \\ Y_3 \end{pmatrix}, \quad \mathbf{Y}_{3,2}^6 = (Y_3^2 + 2Y_1Y_2) \begin{pmatrix} Y_3 \\ Y_1 \\ Y_2 \end{pmatrix}$$

and the total dimension is 7. For $k = 8$, there are

$$\mathbf{Y}_1^8 = (Y_1^2 + 2Y_2Y_3)^2, \quad \mathbf{Y}_{1'}^8 = (Y_1^2 + 2Y_2Y_3)(Y_3^2 + 2Y_1Y_2), \quad \mathbf{Y}_{1''}^8 = (Y_3^2 + 2Y_1Y_2)^2, \\ \mathbf{Y}_{3,1}^8 = (Y_1^2 + 2Y_2Y_3) \begin{pmatrix} Y_1^2 - Y_2Y_3 \\ Y_3^2 - Y_1Y_2 \\ Y_2^2 - Y_1Y_3 \end{pmatrix}, \quad \mathbf{Y}_{3,2}^8 = (Y_3^2 + 2Y_1Y_2) \begin{pmatrix} Y_2^2 - Y_1Y_3 \\ Y_1^2 - Y_2Y_3 \\ Y_3^2 - Y_1Y_2 \end{pmatrix},$$

corresponding to a total dimension of 9 . For $k = 10$, a total of 11 linearly independent modular forms are arranged into A_4 multiplets as

$$\begin{aligned}
\mathbf{Y}_1^{10} &= (Y_1^2 + 2Y_2Y_3) (Y_1^3 + Y_2^3 + Y_3^3 - 3Y_1Y_2Y_3) \\
\mathbf{Y}_{1'}^{10} &= (Y_3^2 + 2Y_1Y_2) (Y_1^3 + Y_2^3 + Y_3^3 - 3Y_1Y_2Y_3) \\
\mathbf{Y}_{3,1}^{10} &= (Y_1^2 + 2Y_2Y_3)^2 \begin{pmatrix} Y_1 \\ Y_2 \\ Y_3 \end{pmatrix}, \quad \mathbf{Y}_{3,2}^{10} = (Y_3^2 + 2Y_1Y_2)^2 \begin{pmatrix} Y_2 \\ Y_3 \\ Y_1 \end{pmatrix} \\
\mathbf{Y}_{3,3}^{10} &= (Y_1^2 + 2Y_2Y_3) (Y_3^2 + 2Y_1Y_2) \begin{pmatrix} Y_3 \\ Y_1 \\ Y_2 \end{pmatrix}.
\end{aligned}$$

B Tensor products of A_4 group in T -diagonal basis

The multiplication rules for the representations of A_4 are as follows

$$1 \otimes 1' = 1', \quad 1'' \otimes 1'' = 1', \quad 1' \otimes 1'' = 1, \quad 1'' \otimes 1 = 1'', \quad 1' \otimes 1' = 1''$$

$$3 \otimes 1' = 3, \quad 3 \otimes 1'' = 3, \quad 3 \otimes 3 = 1 \oplus 1' \oplus 1'' \oplus 3_s \oplus 3_a.$$

In the T -diagonal basis, the Clebsch–Gordan decomposition of two triplets, $m = (m_1, m_2, m_3)$ and $n = (n_1, n_2, n_3)$ is given as

$$\begin{aligned}
(m \otimes n)_1 &= m_1n_1 + m_2n_3 + m_3n_2, \\
(m \otimes n)_{1'} &= m_3n_3 + m_1n_2 + m_2n_1, \\
(m \otimes n)_{1''} &= m_2n_2 + m_1n_3 + m_3n_1, \\
(m \otimes n)_{3_s} &= \frac{1}{3} (2m_1n_1 - m_2n_3 - m_3n_2, 2m_3n_3 - m_1n_2 - m_2n_1, 2m_2n_2 - m_1n_3 - m_3n_1), \\
(m \otimes n)_{3_a} &= \frac{1}{2} (m_2n_3 - m_3n_2, m_1n_2 - m_2n_1, m_1n_3 - m_3n_1).
\end{aligned}$$

References

- [1] I. Esteban, M. C. Gonzalez-Garcia, M. Maltoni, T. Schwetz and A. Zhou, JHEP **09**, 178 (2020).

- [2] M. J. Dolinski, A. W. P. Poon and W. Rodejohann, *Ann. Rev. Nucl. Part. Sci.* **69**, 219-251 (2019).
- [3] M. Roncadelli and D. Wyler, *Phys. Lett. B* **133**, 325-329 (1983).
- [4] S. M. Davidson and H. E. Logan, *Phys. Rev. D* **80**, 095008 (2009).
- [5] M. C. Chen, M. Ratz, C. Staudt and P. K. S. Vaudrevange, *Nucl. Phys. B* **866**, 157-176 (2013).
- [6] N. Memenga, W. Rodejohann and H. Zhang, *Phys. Rev. D* **87**, no.5, 053021 (2013).
- [7] E. Ma and R. Srivastava, *Phys. Lett. B* **741**, 217-222 (2015).
- [8] J. W. F. Valle and C. A. Vaquera-Araujo, *Phys. Lett. B* **755**, 363-366 (2016).
- [9] S. Centelles Chuliá, E. Ma, R. Srivastava and J. W. F. Valle, *Phys. Lett. B* **767**, 209-213 (2017).
- [10] S. Centelles Chuliá, R. Srivastava and J. W. F. Valle, *Phys. Lett. B* **761**, 431-436 (2016).
- [11] M. Reig, J. W. F. Valle and C. A. Vaquera-Araujo, *Phys. Rev. D* **94**, no.3, 033012 (2016).
- [12] S. Centelles Chuliá, R. Srivastava and J. W. F. Valle, *Phys. Lett. B* **773**, 26-33 (2017).
- [13] D. Borah and A. Dasgupta, *JCAP* **06**, 003 (2017).
- [14] C. Bonilla, J. M. Lamprea, E. Peinado and J. W. F. Valle, *Phys. Lett. B* **779**, 257-261 (2018).
- [15] D. Borah and B. Karmakar, *Phys. Lett. B* **780**, 461-470 (2018).
- [16] D. Borah and B. Karmakar, *Phys. Lett. B* **789**, 59-70 (2019).
- [17] D. Borah, D. Nanda and A. K. Saha, *Phys. Rev. D* **101**, no.7, 075006 (2020).
- [18] S. Centelles Chuliá, R. Srivastava and S. Yadav, *Mod. Phys. Lett. A* **38**, no.7, 2350049 (2023).
- [19] H. Ishimori, T. Kobayashi, H. Ohki, Y. Shimizu, H. Okada and M. Tanimoto, *Prog. Theor. Phys. Suppl.* **183**, 1-163 (2010).
- [20] S. F. King, *J. Phys. G* **42**, 123001 (2015).

- [21] A. de Gouvêa, Ann. Rev. Nucl. Part. Sci. **66**, 197-217 (2016).
- [22] G. Chauhan *et al*, [arXiv:2310.20681 [hep-ph]].
- [23] F. Feruglio, [arXiv:1706.08749 [hep-ph]].
- [24] T. Kobayashi, K. Tanaka and T. H. Tatsuishi, Phys. Rev. D **98**, no.1, 016004 (2018).
- [25] T. Kobayashi, Y. Shimizu, K. Takagi, M. Tanimoto, T. H. Tatsuishi and H. Uchida, Phys. Lett. B **794**, 114-121 (2019).
- [26] H. Okada and Y. Orikasa, Phys. Rev. D **100**, no.11, 115037 (2019).
- [27] T. Kobayashi, Y. Shimizu, K. Takagi, M. Tanimoto and T. H. Tatsuishi, PTEP **2020**, no.5, 053B05 (2020).
- [28] S. Marciano, D. Meloni and M. Parriciatu, JHEP **24**, 020 (2020).
- [29] M. K. Behera, P. Ittisamai, C. Pongkitivanichkul and P. Uttayarat, [arXiv:2403.00593 [hep-ph]].
- [30] T. Kobayashi, N. Omoto, Y. Shimizu, K. Takagi, M. Tanimoto and T. H. Tatsuishi, JHEP **11**, 196 (2018).
- [31] P. P. Novichkov, S. T. Petcov and M. Tanimoto, Phys. Lett. B **793**, 247-258 (2019).
- [32] T. Nomura and H. Okada, Phys. Lett. B **797**, 134799 (2019).
- [33] G. J. Ding, S. F. King and X. G. Liu, JHEP **09**, 074 (2019).
- [34] G. J. Ding, S. F. King, X. G. Liu and J. N. Lu, JHEP **12**, 030 (2019).
- [35] T. Kobayashi, Y. Shimizu, K. Takagi, M. Tanimoto and T. H. Tatsuishi, Phys. Rev. D **100**, no.11, 115045 (2019).
- [36] T. Nomura, H. Okada and O. Popov, Phys. Lett. B **803**, 135294 (2020).
- [37] T. Asaka, Y. Heo and T. Yoshida, Phys. Lett. B **811**, 135956 (2020).
- [38] H. Okada and M. Tanimoto, Eur. Phys. J. C **81**, no.1, 52 (2021).
- [39] T. Nomura and H. Okada, Nucl. Phys. B **966**, 115372 (2021).
- [40] P. Mishra, M. K. Behera, P. Panda and R. Mohanta, Eur. Phys. J. C **82**, no.12, 1115 (2022).

- [41] M. K. Behera, S. Singirala, S. Mishra and R. Mohanta, J. Phys. G **49**, no.3, 035002 (2022).
- [42] M. Kashav and S. Verma, JCAP **03**, 010 (2023).
- [43] R. Kumar, P. Mishra, M. K. Behera, R. Mohanta and R. Srivastava, Phys. Lett. B **853**, 138635 (2024).
- [44] M. R. Devi, [arXiv:2303.04900 [hep-ph]].
- [45] S. Centelles Chuliá, R. Kumar, O. Popov and R. Srivastava, Phys. Rev. D **109**, no.3, 035016 (2024).
- [46] J. T. Penedo and S. T. Petcov, Nucl. Phys. B **939**, 292-307 (2019).
- [47] P. P. Novichkov, J. T. Penedo, S. T. Petcov and A. V. Titov, JHEP **04**, 005 (2019).
- [48] I. de Medeiros Varzielas, S. F. King and Y. L. Zhou, Phys. Rev. D **101**, no.5, 055033 (2020).
- [49] T. Kobayashi, Y. Shimizu, K. Takagi, M. Tanimoto and T. H. Tatsuishi, JHEP **02**, 097 (2020).
- [50] S. F. King and Y. L. Zhou, Phys. Rev. D **101**, no.1, 015001 (2020).
- [51] J. C. Criado, F. Feruglio and S. J. D. King, JHEP **02**, 001 (2020).
- [52] X. Wang, Nucl. Phys. B **962**, 115247 (2021).
- [53] P. P. Novichkov, J. T. Penedo, S. T. Petcov and A. V. Titov, JHEP **04**, 174 (2019).
- [54] G. J. Ding, S. F. King and X. G. Liu, Phys. Rev. D **100**, no.11, 115005 (2019).
- [55] G. J. Ding, F. Feruglio and X. G. Liu, SciPost Phys. **10**, no.6, 133 (2021).
- [56] G. J. Ding, F. Feruglio and X. G. Liu, JHEP **01**, 037 (2021).
- [57] S. Kikuchi, T. Kobayashi, K. Nasu, S. Takada and H. Uchida, JHEP **04**, 045 (2024).
- [58] M. Ricky Devi, [arXiv:2401.16257 [hep-ph]].
- [59] N. Aghanim *et al.* [Planck], Astron. Astrophys. **641**, A6 (2020).
- [60] R. L. Workman *et al.* [Particle Data Group], PTEP **2022**, 083C01 (2022).

- [61] A. D. Sakharov, Pisma Zh. Eksp. Teor. Fiz. **5**, 32-35 (1967).
- [62] M. Fukugita and T. Yanagida, Phys. Lett. B **174**, 45-47 (1986).
- [63] T. Asaka, Y. Heo, T. H. Tatsuishi and T. Yoshida, JHEP **01**, 144 (2020).
- [64] M. Kashav and S. Verma, JHEP **09**, 100 (2021).
- [65] M. K. Behera, S. Mishra, S. Singirala and R. Mohanta, Phys. Dark Univ. **36**, 101027 (2022).
- [66] X. Wang and S. Zhou, JHEP **05**, 017 (2020).
- [67] M. K. Behera and R. Mohanta, Front. in Phys. **10**, 854595 (2022).
- [68] D. W. Kang, J. Kim, T. Nomura and H. Okada, JHEP **07**, 050 (2022).
- [69] G. J. Ding, S. F. King, J. N. Lu and B. Y. Qu, JHEP **10**, 071 (2022).
- [70] K. Dick, M. Lindner, M. Ratz and D. Wright, Phys. Rev. Lett. **84**, 4039-4042 (2000).
- [71] M. Boz and N. K. Pak, Eur. Phys. J. C **37**, 507-510 (2004).
- [72] B. Thomas and M. Toharia, Phys. Rev. D **73**, 063512 (2006).
- [73] P. H. Gu and H. J. He, JCAP **12**, 010 (2006).
- [74] A. Bechinger and G. Seidl, Phys. Rev. D **81**, 065015 (2010).
- [75] M. C. Chen, J. Huang and W. Shepherd, JHEP **11**, 059 (2012).
- [76] K. Y. Choi, E. J. Chun and C. S. Shin, Phys. Lett. B **723**, 90-94 (2013).
- [77] D. Borah and A. Dasgupta, JCAP **12**, 034 (2016).
- [78] P. H. Gu, JCAP **07**, 004 (2016).
- [79] N. Narendra, N. Sahoo and N. Sahu, Nucl. Phys. B **936**, 76-90 (2018).
- [80] J. Lauer, J. Mas and H. P. Nilles, Phys. Lett. B **226**, 251-256 (1989).
- [81] W. Lerche, D. Lust and N. P. Warner, Phys. Lett. B **231**, 417-424 (1989).
- [82] J. Lauer, J. Mas and H. P. Nilles, Nucl. Phys. B **351**, 353-424 (1991).
- [83] D. Cremades, L. E. Ibanez and F. Marchesano, JHEP **05**, 079 (2004).

- [84] P. P. Novichkov, J. T. Penedo and S. T. Petcov, JHEP **03**, 149 (2022)
- [85] S. F. King and X. Wang, [arXiv:2310.10369 [hep-ph]].
- [86] T. Kobayashi and S. Nagamoto, Phys. Rev. D **96**, no.9, 096011 (2017).
- [87] P. I. Krastev and S. T. Petcov, Phys. Lett. B **205**, 84-92 (1988).
- [88] C. Jarlskog, Phys. Rev. Lett. **55**, 1039 (1985).
- [89] K. Abe *et al.* [T2K], Nature **580**, no.7803, 339-344 (2020).
- [90] K. Abe *et al.* [T2K], Phys. Rev. D **103**, no.11, 112008 (2021).
- [91] K. Abe *et al.* [T2K], Eur. Phys. J. C **83**, no.9, 782 (2023).
- [92] V. A. Kuzmin, V. A. Rubakov and M. E. Shaposhnikov, Phys. Lett. B **155**, 36 (1985).
- [93] G. F. Giudice, A. Notari, M. Raidal, A. Riotto and A. Strumia, Nucl. Phys. B **685**, 89-149 (2004).
- [94] S. Marciano, D. Meloni and M. Parriciatu, [arXiv:2402.18547 [hep-ph]].
- [95] A. Abada, S. Davidson, F. X. Josse-Michaux, M. Losada and A. Riotto, JCAP **04**, 004 (2006).
- [96] E. Nardi, Y. Nir, E. Roulet and J. Racker, JHEP **01**, 164 (2006).
- [97] A. Abada, S. Davidson, A. Ibarra, F. X. Josse-Michaux, M. Losada and A. Riotto, JHEP **09**, 010 (2006).
- [98] S. Blanchet and P. Di Bari, JCAP **03**, 018 (2007).
- [99] D. G. Cerdeno, A. Dedes and T. E. J. Underwood, JHEP **09**, 067 (2006).